Chapter 2
Recent and Future Changes in the Meteorology of the Pacific Arctic

James E. Overland, Jia Wang, Robert S. Pickart, and Muyin Wang

Abstract The meteorology of the Pacific Arctic (the Bering Sea through the Chukchi and southern Beaufort Seas) represents the transition zone between the moist and relatively warm maritime air mass of the Pacific Ocean to the cold and relatively dry air mass of the Arctic. The annual cycle is the dominant feature shifting from near total darkness with extensive sea ice cover in winter to solar heating in summer that is equal to that of sub-tropical latitudes. Strong north-south gradients in air temperatures and sea level pressure are typical over the Pacific Arctic giving rise to climatological polar easterly winds (blowing from the east) throughout the year. Localized storms (regions of low sea level pressure) can propagate into the region from the south but high pressure regions are typical, connected to either northeastern Siberia or the southern Beaufort Sea. The northern portion of the Pacific Arctic has participated in the general Arctic-wide warming in all seasons over the last decade while the southern Bering Sea turned to near record cold temperatures after 2006. Future climate changes in the Pacific Arctic will come from shifts in the timing and extent of seasonal sea ice. Based on climate model projections, cold and dark conditions will still dominate over a climate warming scenario in the Bering Sea of +2 °C by 2050. The northern Bering Sea will continue to have

J.E. Overland (✉)
Pacific Marine Environmental Laboratory, National Oceanic and Atmospheric Administration, 7600 Sand Point Way NE, Seattle, WA 98115, USA
e-mail: james.e.overland@noaa.gov

J. Wang
Great Lakes Environmental Research Laboratory (GLERL), National Oceanic and Atmospheric Administration, Ann Arbor, MI, USA
e-mail: jia.wang@noaa.gov

R.S. Pickart
Woods Hole Oceanographic Institution, Woods Hole, MA 02543, USA

M. Wang
Joint Institute for the Study of the Atmosphere and Ocean, University of Washington, Seattle, WA 98195, USA

J.M. Grebmeier and W. Maslowski (eds.), *The Pacific Arctic Region: Ecosystem Status and Trends in a Rapidly Changing Environment*, DOI 10.1007/978-94-017-8863-2_2,

extensive sea ice January through April, while the southern shelf will have on average less sea ice than currently observed but with large interannual variability. The largest change has the southern Chukchi Sea shifting from being sea ice free in September and October at present to becoming sea ice free for 5 months from July through November within a decade or two, impacting shipping, oil exploration, and ecosystems.

Keywords Arctic meteorology • Siberian high • Aleutian low • Arctic Oscillation • Climate change • Sea ice • Bering Sea • Chukchi Sea

2.1 Introduction

In this atmospheric review, the Pacific Arctic covers the area from the Bering Sea south of St. Lawrence Island north through Bering Strait to the southern Chukchi and Beaufort Seas. This is the transition zone between the relatively warm and moist storm tracks of the Aleutian low weather system in the south to the cold, dry and high pressure Arctic air mass to the north. This is a region of large north-south gradients in atmospheric properties such as air temperature and atmospheric sea level pressure (SLP). The region of strongest gradients moves north and south with the seasonal cycle. Maximum temperature gradients in winter are over the central Bering Sea with sub-freezing temperatures and sea ice coverage. In summer, the strongest air temperature gradients are across the Chukchi Sea and along the north slope and seaward of the coast of Alaska with temperatures above freezing. Large gradients in SLP produce an east-west region of strong wind speeds in all seasons; for example the annual mean surface wind speed at Barrow, Alaska for 1972–2007 is 5.6 m s^{-1} (Wendler et al. 2010).

The causes for the meteorology of the Pacific Arctic region are a seasonal swing from a large heat loss in winter and the dominating presence of sea ice to a gain of heat in summer. The primary determinant of this seasonal climate shift is the annual cycle of insolation from a maximum of 500 W m^{-2} near the summer solstice to darkness in winter. As summer progresses, absorption of insolation at the ocean surface increases as the albedo decreases due to snow and ice melt and increased open water areas. This annual cycle results in a change from a winter continental-like air mass similar to the adjacent land areas to a summertime marine air mass characterized by low clouds and fog.

In the recent decade, the Pacific air mass to the south and the Arctic air mass to the north appear to be on different climate change trajectories (Overland et al. 2012). To the north, the region is part of the decadal change of Arctic warming where recent sea ice losses are changing the climatology of the region, with periods of warm temperature anomalies extending through the autumn months. To the south, the Bering Sea has turned cold with extensive sea ice cover in 2007–2011, extents that had not been seen since the mid-1970s. This contrasts to a warmer than normal temperature anomaly period for the southern Bering Sea from 2001 through

2005. This north-south decoupling is due to the northern region being dominated by the thermodynamics of melting sea ice, while changes in the south are dominated by changes in North Pacific storm tracks and large-scale Pacific climate.

2.2 Climatological Fields

The basic driver of Pacific Arctic meteorology is the annual cycle of solar insolation (Fig. 2.1). Although the sun is close to the horizon during summer, the 24 h of daylight provides the same potential solar radiation (i.e., without cloud effects) in the Arctic as occurs at lower latitudes in the northern hemisphere. North of 60°N, there is substantial solar heating from mid-April through August.

Climatologically, in terms of surface air temperature (SAT) and SLP gradients, the Pacific Arctic can be considered to have two main seasons: an extended 9-month winter (September through May) and a summer (June through August). This is demonstrated by examining the SAT fields for standard seasons, fall (Sept–Nov), winter (Dec–Feb), spring (Mar–May) and summer (Jun–Aug), presented in Fig. 2.2. Strong north-south temperature gradients are present fall through spring from northern Alaska southward through the southeastern Bering Sea. In summer, more efficient heating of the continental land masses changes the orientations of the isotherms so that a sea-land temperature gradient occurs over the coastal regions of northwestern Alaska and eastern Siberia. For the SLP fields (Fig. 2.3), during fall through spring, the Aleutian low pressure center is dominant over southwestern Alaska, with the strongest pressure gradient occurring in the vicinity of Bering Strait. The strength of SLP gradient over the Pacific Arctic is greatest in

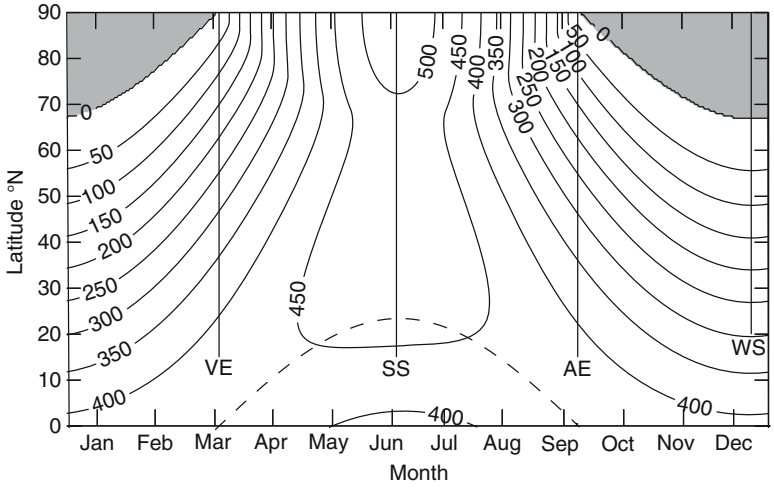

Fig. 2.1 The daily variation of solar insolation at the top of the atmosphere as a function of latitude and day of year in units of Wm^{-2} for the Northern Hemisphere (Modified from Liou 2002)

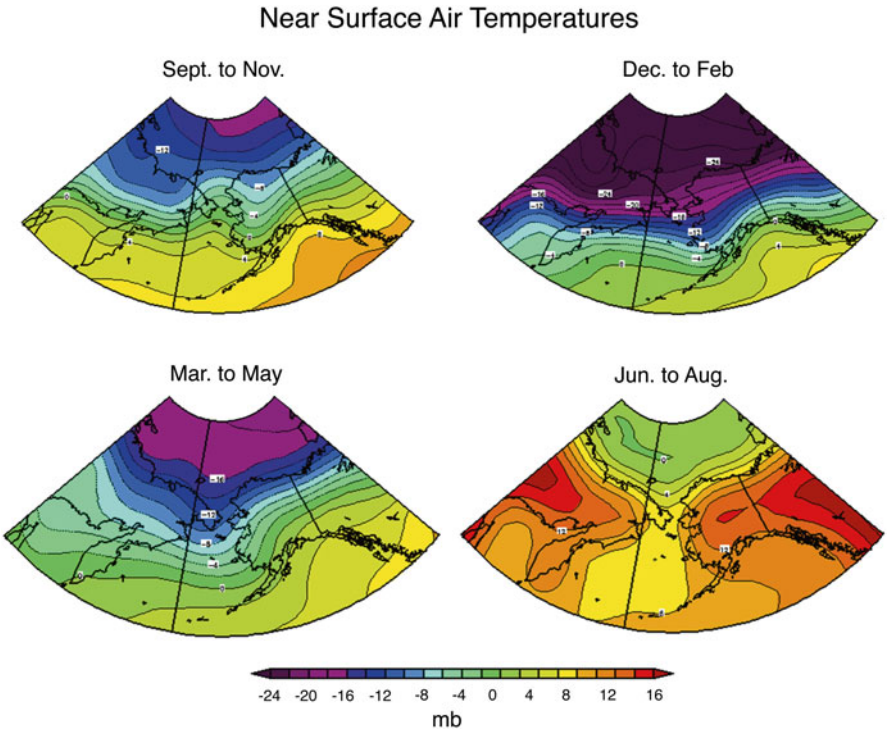

Fig. 2.2 Mean (1961–2010) near-surface temperature (°C) for the four seasons over the Pacific Arctic (Data are from the NCEP–NCAR Reanalysis through the NOAA/Earth Systems Research Laboratory, generated online at: http://www.esrl.noaa.gov/psd/cgi-bin/data/composites/printpage.pl)

winter. Climatological winds are easterly (from the east) and their magnitude drops off rapidly in the northern Chukchi Sea. In summer, the climatological SLP field is nearly flat. Typically, small storms can be produced along the temperature gradient in northern Alaska and these can drift out into the Chukchi/Beaufort Seas (Serreze et al. 2001). For a more detailed review of the marine climatology of the Beaufort Sea proper see Overland (2009).

2.3 Storms and Temporal Variability

The Pacific Arctic is dominated by high SLP regions for most of the year. These are large and slow-moving systems that persist for multiple days. The center of one of these systems is the Siberian high, far to the west. However, the edge of the high, where strong pressure gradients exist, can reside over the Pacific Arctic region, producing strong and persistent northwesterly or northeasterly winds. The other

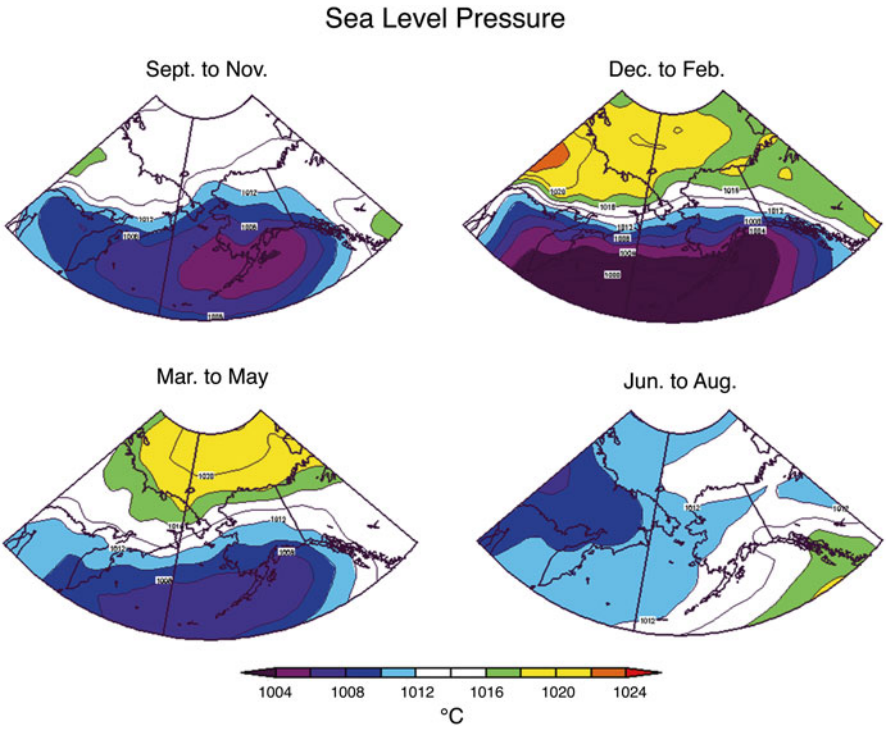

Fig. 2.3 Mean (1961–2010) sea level pressure (*SLP*) for the four seasons over the Pacific Arctic (Data are from the NCEP–NCAR Reanalysis through the NOAA/Earth Systems Research Laboratory, generated online at: http://www.esrl.noaa.gov/psd/cgi-bin/data/composites/printpage.pl)

high pressure center is over the Canadian Beaufort Sea. If there is very low pressure to the south of the region in the form of Aleutian low storm systems, there can be stronger than average easterly winds across northern Alaska and adjacent waters. These east wind events can cause coastal ocean upwelling events across the narrow northern Alaskan continental shelf (Nikolopoulos et al. 2009).

Storm track trajectories originating in the northwest Pacific and moving into the Pacific Arctic are generally of two types (Wang et al. 2004; Pickart et al. 2009). One type exhibits a west-to-east trajectory south of the region and may increase the north-south pressure gradient as the low pressure region passes to the south of the more permanent higher pressure zones to the north (Fig. 2.4). The second trajectory type curves northward from the south into the central Bering Sea. Conventional wisdom at the Anchorage NOAA Weather Service is that a sequence of storms on this latter trajectory would continue to progress farther north displacing the northern high pressure centers. The first storm would make it to the central Bering Sea, the second storm would intrude to north of Bering Strait, and the third would transit Bering Strait and then curve eastward along the northern slope of Alaska.

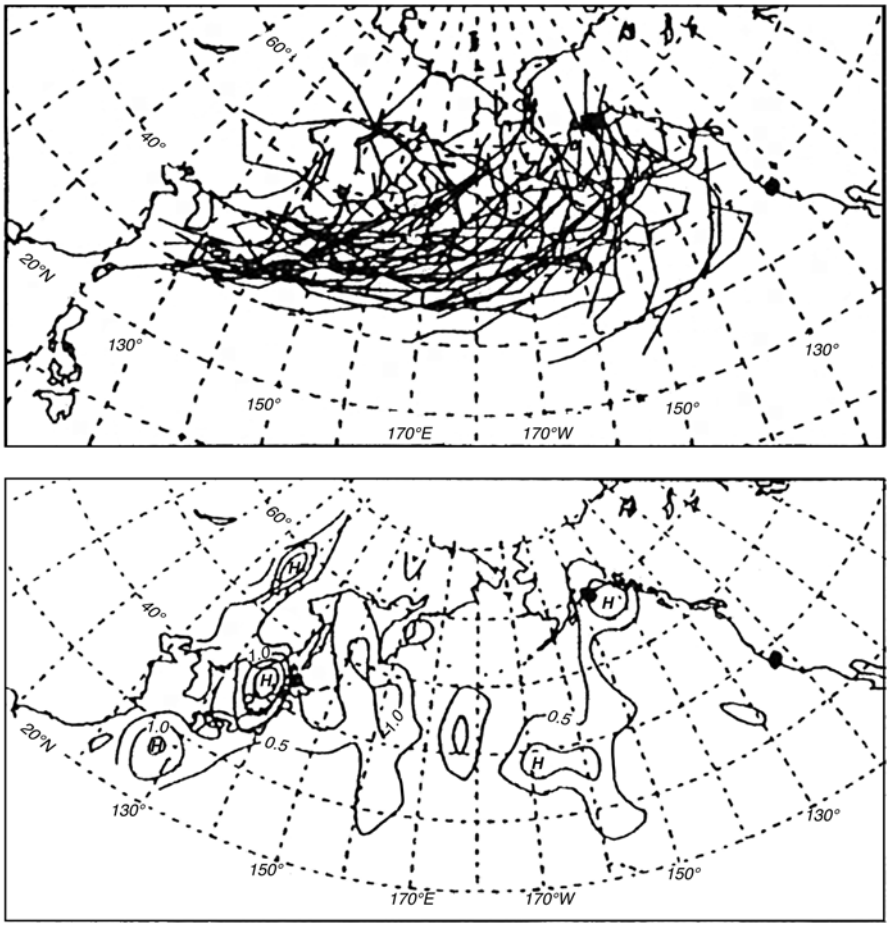

Fig. 2.4 Cyclone (storm) tracks during a typical wet season (October 1979–May 1980). A total of 57 cyclones were found during this period (*upper panel*). Cyclogenesis (storm development) location distribution is also shown for January 1980 (*lower panel*, units are in cyclones/month, with interval being 0.05) (After Wang et al. 2004)

The lower troposphere of the Pacific Arctic (eastern Siberia to northern Canada) was relatively warm during spring in the 1990s relative to the previous four decades (Overland et al. 2002). The primary difference in the 1990s was the presence of several highly episodic springtime storms and associated advection of heat compared to nearly storm-free periods in previous years. Krupnik and Jolly (2002) note that native elders in the region suggested that the weather was less dependable (predictable) starting in the 1990s. The addition of a few storms that propagated further north may be a cause of this diminished predictability relative to previous persistent easterly winds.

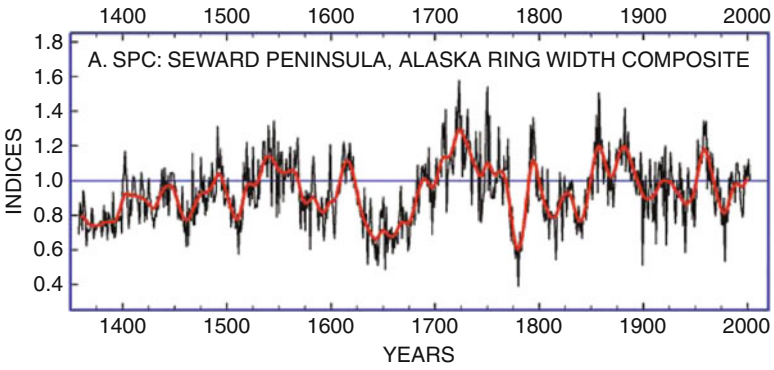

Fig. 2.5 Ring-width composite chronology extending from 1358 to 2001 A.D. A 25-year smoothing spline (*red line*) has been superimposed on this record to emphasize multi-decadal-scale fluctuations (After D'Arrigo et al. 2005)

Such changes, however, may have begun as early as the late 1960s or at least by the well-known Alaskan regime shift in the 1970s (Wang et al. 2006; Wendler et al. 2010). Before the 1960s, Barrow and Nome were dominated by Arctic air masses and St. Paul was dominated by North Pacific maritime air masses. After the 1960s, the surface air temperature correlation in winter between Barrow and St. Paul increased from 0.2 to 0.7 and between Nome and St. Paul from 0.4 to 0.8, implying greater north–south penetration of both Arctic and Pacific air masses. Relatively stable, high correlations are found among the stations in the fall, whereas correlations are low in the summer. These climatological results support the concept that the southeast Bering Sea ecosystem may have been dominated by Arctic species for most of the twentieth century, with a gradual replacement by sub-Arctic species, such as pollock, in the last 30 years (Aydin et al. 2007).

The opening date for the Prudhoe Bay shipping season depends on antecedent sea ice and weather conditions in the Bering Sea (Drobot et al. 2009). In years with early opening dates, the sea-ice cover in the southern Bering Sea is reduced in February and, as the season progresses, sea-ice concentrations in the central and northern Bering Sea remain low. Further, fewer accumulated freezing degree days (FDDs) suggests that temperatures are warmer over a broad area, ranging from the Bering Sea through the Chukchi Sea and the Beaufort Sea, in winter and spring months preceding early opening dates.

Based on tree ring widths of 14 white spruce chronologies for the Seward Peninsula, Alaska, some historical changes can be inferred for the Pacific Arctic back to 1400 (D'Arrigo et al. 2005). The chronologies correlate significantly with Bering and Chukchi Sea sea surface temperatures and with the Pacific Decadal Oscillation index weighted towards the spring and summer months. There is inferred cooling during periods within the Little Ice Age (LIA) from the early-to-middle 1600s and from the early-to-late 1700s, and warming from the middle 1600s to early 1700s (Fig. 2.5). The chronologies imply that growth conditions were

somewhat below average until the middle of the twentieth century. Following a brief period of increasing growth in the 1950s, there is a decline, with some growth recovery in the 1990s.

2.4 The Differences of the Pacific Sector Relative to the Larger Arctic System

The largest climate signal for the Pacific Arctic in the recent decade is the apparent decoupling of trends in the marine air masses to the south and Arctic air masses. Major temperature increases are seen in the Arctic related to sea ice loss in the summer and subsequent positive temperature anomalies in the fall. In contrast, southern Bering Sea warming in 2001–2005 and subsequent cooling 2007–2012 are tied to sea surface temperature shifts in the North Pacific. A long-term, vertically-averaged ocean temperature record from the M2 mooring (Stabeno et al. 2012; Fig. 2.6) on the southeastern Bering shelf illustrate these warming and cooling trends. The annual average temperature anomaly chart (Fig. 2.7) for 2006 through 2012 shows extensive large positive temperature anomalies over much of the Arctic, with a cooling in the southeastern Bering Sea. The large-scale warming of the Arctic is evident in all months north of St. Lawrence Island, but is most pronounced in the autumn.

The warming in the Arctic appears to be associated with the recent predominance of a climate pattern referred to as the Arctic Dipole (AD), characterized by low SLP on one side of the Arctic and high SLP on the other (Overland and Wang 2005; Wang et al. 2009; Zhang et al. 2008). On a hemispheric basis, the AD occurs as the third most prominent pattern after the Arctic Oscillation (AO) pattern, which has low SLP over the central Arctic in its positive phase, and the Pacific North-American pattern (Overland et al. 2008). While the AD was present in spring as early as 1997, its recent occurrence began in summer 2007 when it was present in all months and contributed to 2007 record minimum summer sea ice extent (Fig. 2.8). Each year after 2007 has also seen the AD pattern for part of the summer. For example, in 2010, the AD pattern was present in May and June, but then the Arctic reverted to the more traditional climatological SLP pattern for summer of a weak, relatively small low-pressure center. However, by August 2010 the AD pattern had returned.

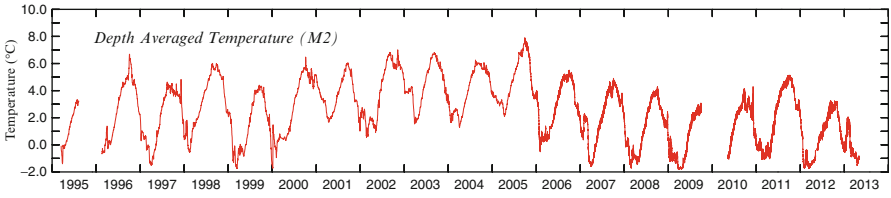

Fig. 2.6 Depth averaged ocean temperature at the M2 mooring location on the southeastern Bering Sea shelf (Updated from Stabeno et al. 2012)

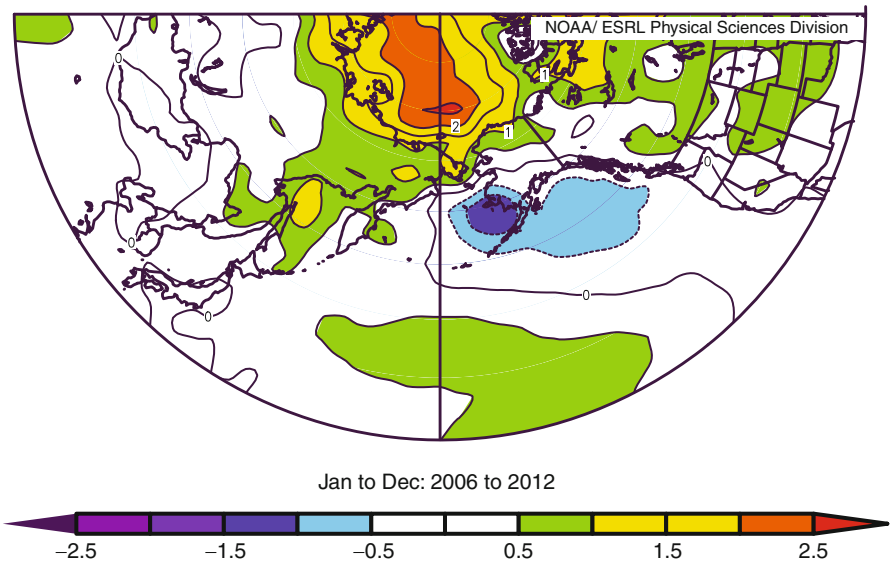

Fig. 2.7 Near surface air temperature anomaly multiyear composites (°C) for 2006–2012. Anomalies are relative to 1981–2010 mean and show a strong Arctic amplification of recent temperature trends and cooling of the southeastern Bering Sea (Data are from the NCEP–NCAR Reanalysis through the NOAA/Earth Systems Research Laboratory, generated online at: http://www.esrl.noaa.gov/psd/cgi-bin/data/composites/printpage.pl)

2.5 The Future Climate of the Pacific Arctic

The anthropogenic contribution to a warming Arctic is estimated to be 4–6 °C by 2080 (Chapman and Walsh 2007). Climate models also predict that the Arctic Ocean will be nearly sea ice free during the summer before the second half of this century, but recent data on thinning of Arctic sea ice suggest that the loss of Arctic summer sea ice may occur much sooner, within a decade or so (Stroeve et al. 2008; Wang and Overland 2009, 2012; Overland and Wang 2013). The Pacific Arctic is essentially sea ice free in summer at the present time. Such an occurrence will be limited to summer, since during the cold season, the Arctic Ocean, with its lack of sun light, will continue to be an ice covered sea.

As the Bering Sea is sea ice free in summer, it is characterized not by summer minima, but rather by winter/spring sea ice maxima. During the winters and springs of 2008–2013, there were near record maximum sea-ice extents in the southeastern Bering Sea. This contrasts with the record 2007–2012 summer Arctic sea ice minima and suggests a lack of continuity or "decoupling" between summer sea ice minima in the Arctic and the eventual winter/spring sea-ice maxima in the Bering Sea for the following season. This is a result of the main thermodynamic physics at high latitudes; it is cold and dark in winter. The northern Bering Sea (at 64°N) has only 4 h of daylight at the winter solstice. Mean monthly maximum temperatures at

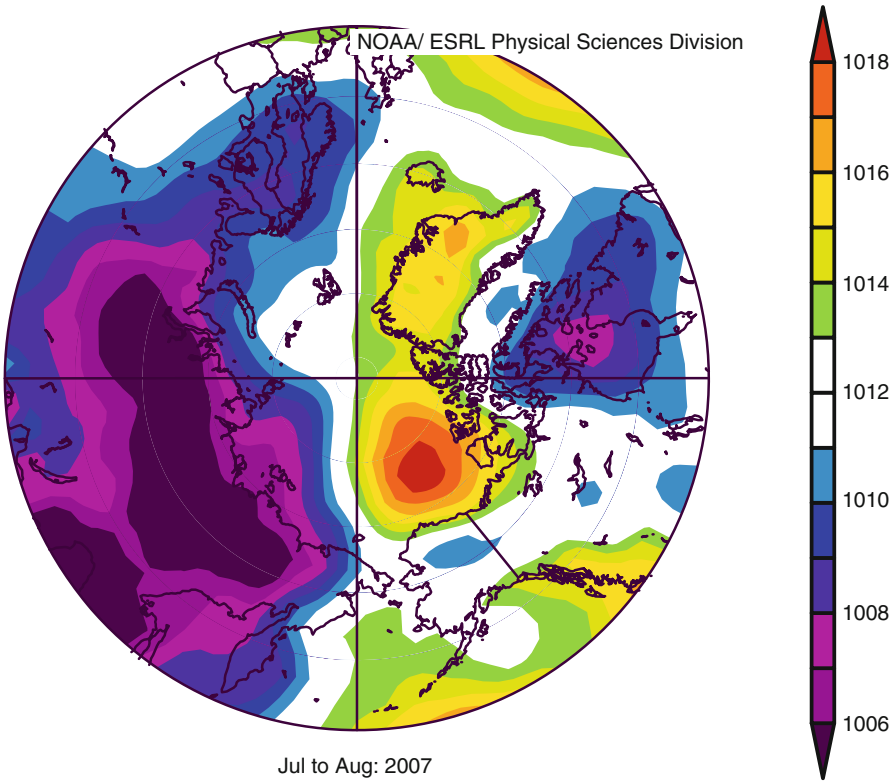

Fig. 2.8 Sea level pressure (*SLP*) field corresponding to the minimum sea ice extent in summer 2007 showing the Arctic Dipole (*AD*) pattern (Data are from the NCEP–NCAR Reanalysis through the NOAA/Earth Systems Research Laboratory, generated online at: www.cdc.noaa.gov)

Nome, Alaska, averaged from 1949 through 2006, are below −2.9 °C for all months between November and April indicating freezing conditions during these months. Mean maximum temperatures in these months will stay below freezing even with a hypothesized regional increased of 2 °C due to an overall global warming signal by 2050. Thus, winter and spring conditions in the western Arctic should not be dissimilar than current conditions for the foreseeable future.

We have some confidence for using climate models from the Intergovernmental Panel on Climate Change fourth Assessment Report (now referred to as CMIP3 and updated to CMIP5) to project April, May and November sea ice areas (Overland and Wang 2007). Figure 2.9 shows the observed area of sea ice cover (black lines) in the eastern Bering Sea for April and May for past years. May, in particular, has considerable year-to-year variability with extensive sea ice coverage in the mid-1970s. The blue line is the composite mean projection of 12 CMIP5 models (ACCESS1.0, ACCESS1.3, CCSM4, CESM1-CAM5.1, EC-EARTH, HadGEM2-AO, HadGEM2-CC, HadGEM2-ES, MIROC-ESM-CHEM, MIROC-ESM,

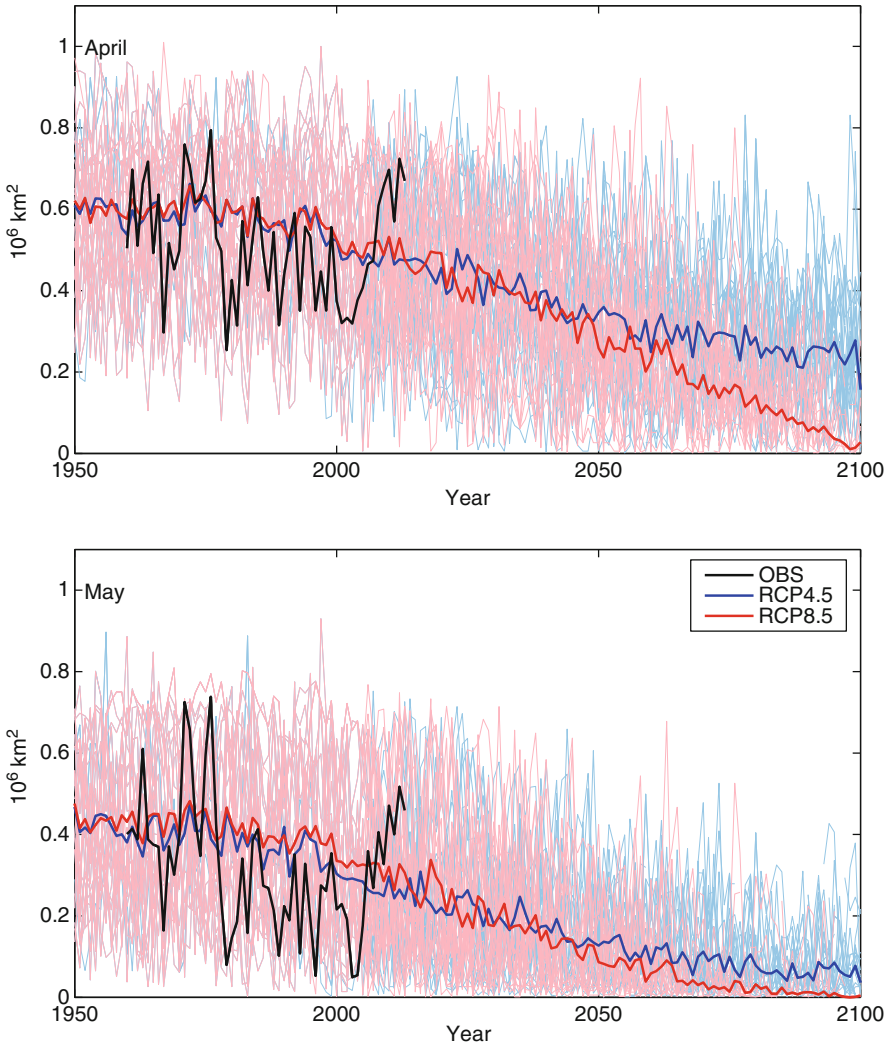

Fig. 2.9 April and May sea ice extent over the eastern Bering Sea based on HadleyISST_ice analysis (*black line*) and projections from CMIP5 models. *Thin colored lines* are individual model projections from 12 models that simulate the Arctic sea ice extent well in their historical simulations (Updated from Wang and Overland 2012). The *thick colored lines* are the ensemble mean value for each year averaged over these individual projections under RCP4.5 (*blue*) and RCP8.5 (*red*) emissions scenarios

MPI-ESM-LR, and MPI-ESM-MR.) which simulate well the mean and magnitude of seasonal cycle of sea ice coverage during 1981–2005 period. The thin blue/pink curves in the background represent multiple single runs (ensemble members) of the 12 selected models and suggest the possible range of future sea-ice areal coverage due to the influence of natural variability and to the anthropogenic

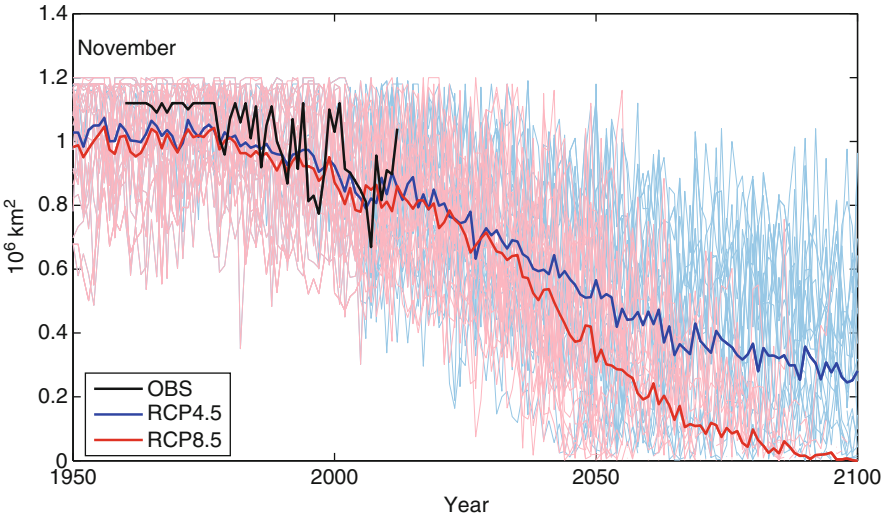

Fig. 2.10 November sea ice extent over the Chukchi Sea based on HadleyISST_ice analysis (*black line*) and projections from 12 CMIP5 models. *Light colored lines* are individual model projections from these models under RCP4.5 (*blue*) and RCP8.5 (*pink*) emissions scenarios. The *thick colored line* are the ensemble mean value for each year averaged over these individual projections under RCP4.5 (*blue*) and RCP8.5 (*red*) emissions scenarios

contribution represented by the thick blue and red lines under proposed emissions scenarios. These results from CMIP5 models show similar results to CMIP3 for the Pacific Arctic (Wang et al. 2012).

While there are measurable decreases in mean sea-ice areal estimates in April after 2010, the individual simulations (blue/pink lines) suggest that it is unlikely for the Bering Sea to be ice free in April during this century. In contrast, in May, the ensemble mean sea-ice area (blue line) decreases to 56 % of the 1960–1980 average area by 2100. The observations for May (black line) show many years in recent decades which approach a near-zero sea-ice areal coverage, but there are still individual model simulations from 2010 to 2050 where the sea-ice coverage exceeds the historical coverage from 1980 to the present. The trend toward minimal ice coverage can be expected to continue, but significant ice cover in May during any given year remains a distinct possibility through at least 2050. The main message from Fig. 2.9 is that large interannual variability in sea ice cover will continue to dominate the eastern Bering Sea in May for the next 40 years.

In contrast to spring sea ice conditions in the eastern Bering Sea, we project large changes in sea ice cover for the Chukchi Sea in autumn. Even for November, we see future reductions in sea ice coverage (Fig. 2.10). As in the Bering Sea, the range of individual ensemble members (blue/pink lines) is large, showing the uncertainty due to natural variability relative to the global warming signal. Loss of November sea ice cover has major implications for potential shipping and resource

exploration, as well as overall ecosystem shifts including habitat changes for marine mammals. For the southern Chukchi Sea there is a shift from September and October being sea ice free at the present time to July through November being sea ice free within a decade or two.

2.6 Summary

The Pacific Arctic is not characterized by uniformity, but by its large north-south differences in marine habitats. Strong north-south gradients in air temperature and sea level pressure are established by latitudinal differences in the annual cycle of solar insolation. An anthropogenic temperature increase of 2 ° C by 2050 will have only a modest impact on the Bering Sea which will still be characterized by large interannual variability in addition to the weak upward temperature trend and a decreasing sea ice extent. Because of the unique thermodynamic influences of sea ice (albedo changes and ocean heat storage in newly sea-ice free areas), loss of autumnal sea ice will continue to provide major changes in the Chukchi Sea through November over the next decades with major increases in economic access and ecological impacts.

Acknowledgements We appreciate the support from NOAA Arctic Research of the NOAA Climate Program Office. This publication is partially funded by the Joint Institute for the Study of the Atmosphere and Ocean (JISAO) under NOAA Cooperative Agreement No. NA10OAR4320148 (M. Wang), Contribution No.2168. PMEL contribution #2679. We also like to thank EcoFOCI program of PMEL who maintains M2 mooring on the Bering Sea shelf.

References

Aydin K, Gaichas S, Ortiz I, Kinzey D, Friday N (2007) A comparison of the Bering Sea, Gulf of Alaska, and Aleutian Islands large marine ecosystems through food web modeling, NOAA technical memorandum 2007 NMFS-AFSC-178. U.S. Department of Commerce, Seattle, 298 pp

Chapman WL, Walsh JE (2007) Simulations of Arctic temperature and pressure by global coupled models. J Clim 20:609–632

D'Arrigo R, Mashig E, Frank D, Wilson R, Jacoby G (2005) Temperature variability over the past millennium inferred from Northwestern Alaska tree rings. Clim Dyn 24:227–236

Drobot SD, Maslanik JA, Anderson MR (2009) The Arctic frontal zone as seen in the NCEP–NCAR reanalysis. Int J Climatol 29:197–203

Krupnik I, Jolly D (2002) The earth is faster now. Arctic Research Consortium of the United States, Fairbanks

Liou KN (2002) An introduction to atmospheric radiation. Academic Press, Amsterdam/Boston

Nikolopoulos A, Pickart RS, Fratantoni PS, Shimada K, Torres DJ, Jones EP (2009) The western Arctic boundary current at 152 W: structure, variability, and transport. Deep Sea Res II Top Stud Oceanogr 56:1164–1181

Overland JE (2009) Meteorology of the Beaufort Sea. J Geophys Res 114:C00A07. doi:10.1029/2008JC004861

Overland JE, Wang M (2005) The third Arctic climate pattern: 1930s and early 2000s. Geophys Res Lett 32:L23808. doi:10.1029/2005GL024254
Overland JE, Wang M (2007) Future regional Arctic Sea ice declines. Geophys Res Lett 34:L17705. doi:10.1029/2007GL030808
Overland JE, Wang M (2013) When will the summer Arctic be nearly sea ice free? Geophys Res Lett 40:2097–2101. doi:10.1002/grl.50316
Overland JE, Bond NA, Adams JM (2002) The relation of surface forcing of the Bering Sea to large-scale climate patterns. Deep Sea Res II Top Stud Oceanogr 49:5855–5868
Overland JE, Wang M, Salo S (2008) The recent Arctic warm period. Tellus 60A:589–597
Overland JE, Wang M, Wood KR, Percival DB, Bond NA (2012) Recent Bering Sea warm and cold events in a 95-year perspective. Deep-Sea Res II 65–70:6–13. doi:10.1016/j.dsr2.2012.02.013
Pickart RS et al (2009) Seasonal evolution of Aleutian low pressure systems: implications for the North Pacific subpolar circulation. J Phys Oceanogr 39:1317–1339
Serreze MC, Lynch AH, Clark MP (2001) The Arctic frontal zone as seen in the NCEP–NCAR reanalysis. J Clim 14:1550–1567
Stabeno PJ et al (2012) Comparison of warm and cold years on the southeastern Bering Sea shelf and some implications for the ecosystem. Deep-Sea Res II 65–70:31–45. doi:10.1016/j.dsr2.2012.02.020
Stroeve JM, Serreze M, Drobot S, Gearheard S, Holland M, Maslanik J, Meier W, Scambos T (2008) Arctic sea ice extent plummets in 2007. EOS Trans Am Geophys Union 89:13–14
Wang M, Overland JE (2009) A sea ice free summer Arctic within 30 years? Geophys Res Lett 36:L07502. doi:10.1029/2009GL037820
Wang M, Overland JE (2012) A sea ice free summer Arctic within 30 years-an update from CMIP5 models. Geophys Res Lett 39:L18501. doi:10.1029/2012GL052868
Wang J, Jin M, Musgrave D, Ikeda M (2004) A numerical hydrological digital elevation model for freshwater discharge into the Gulf of Alaska. J Geophys Res 109:C07009. doi:10.1029/2002JC001430
Wang M, Overland JE, Percival D, Mofjeld HO (2006) Change in the Arctic influence on Bering Sea climate during the twentieth century. Int J Climatol 26:531–539
Wang J et al (2009) Is the Dipole Anomaly a major driver to record lows in Arctic summer sea ice extent? Geophys Res Lett 36:L05706. doi:10.1029/2008GL036706
Wang M, Overland JE, Stebeno P (2012) Future climate of the Bering and Chukchi Seas projected by global climate models. Deep-Sea Res II 65–70:46–57
Wendler G, Shulsk M, Moore B (2010) Changes in the climate of the Alaskan North Slope and the ice concentration of the adjacent Beaufort Sea. Theor Appl Climatol 99:67–74
Zhang X, Sorteberg A, Zhang J, Gerdes R, Comiso J (2008) Recent radical shifts in atmospheric circulations and rapid changes in Arctic climate system. Geophys Res Lett 35:L22701. doi:10.1029/2008GL035607

http://www.springer.com/978-94-017-8862-5

The Pacific Arctic Region
Ecosystem Status and Trends in a Rapidly Changing Environment
Grebmeier, J.M.; Maslowski, W. (Eds.)
2014, XV, 450 p. 153 illus., 129 illus. in color.,
Hardcover
ISBN: 978-94-017-8862-5